RSC Advances

PAPER

View Article Online
View Journal | View Issue

Cite this: *RSC Adv.*, 2022, **12**, 3948

Alkali metal decorated C_{60} fullerenes as promising materials for delivery of the 5-fluorouracil anticancer drug: a DFT approach†

Mehdi D. Esrafili *[a] and Adnan Ali Khan [bc]

The development of effective drug delivery vehicles is essential for the targeted administration and/or controlled release of drugs. Using first-principles calculations, the potential of alkali metal (AM = Li, Na, and K) decorated C_{60} fullerenes for delivery of 5-fluorouracil (5FU) is explored. The adsorption energies of the 5FU on a single AM atom decorated C_{60} are −19.33, −16.58, and −14.07 kcal mol^{-1} for AM = Li, Na, and K, respectively. The results, on the other hand, show that up to 12 Li and 6 Na or K atoms can be anchored on the exterior surface of the C_{60} fullerene simultaneously, each of which can interact with a 5FU molecule. Because of the moderate adsorption energies and charge-transfer values, the 5FU can be simply separated from the fullerene at ambient temperature. Furthermore, the results show that the 5FU may be easily protonated in the target cancerous tissues, which facilitates the release of the drug from the fullerene. The inclusion of solvent effects tends to decrease the 5FU adsorption energies in all 5FU-fullerene complexes. This is the first report on the high capability of AM decorated fullerenes for delivery of multiple 5FU molecules utilizing a C_{60} host molecule.

Received 18th December 2021
Accepted 23rd January 2022

DOI: 10.1039/d1ra09153k

rsc.li/rsc-advances

1. Introduction

It is generally accepted that the mode of administration and dose of a drug have a significant impact on its efficacy. By discovering a variety of drug delivery systems (DDSs), it is now feasible to better regulate the pharmacokinetics, pharmacodynamics, toxicity, immunogenicity, and efficacy of medications.[1–3] DDSs are developed technologies that allow for the targeted administration and/or controlled release of therapeutic drugs.[4,5] In recent decades, DDSs based on nanotechnology have attracted substantial attention due to their essential role in improving the pharmacological properties and bioavailability of different medicines.[6–9] Drugs can be adsorbed or conjugated onto the surface of nanoparticles, encapsulated in the core, or dissolved inside the particle matrix in nanodelivery systems.[10,11] By incorporating targeting moieties onto the particle surface, drug-loaded nanoparticles may be further tailored to a specific disease site. DDSs based on nanostructures offer several advantages, including increased drug stability and water solubility, extended cycle duration, improved absorption rate of target cells or tissues, and reduced enzyme degradation, all of which improve drug safety and efficacy.[12–14]

Nanotechnology has been proven to bridge the gap between biological and physical sciences by employing nanostructures in a variety of scientific areas such as drug delivery and nanomedicine.[15,16] Carbon nanostructures have inspired significant scientific interest in recent decades due to their unusual and extraordinary properties in comparison to typical bulk materials. They have been used in a variety of disciplines, including electronics, sensing, catalysis, gas storage and the environment.[17–24] The high surface-to-volume ratio, superior mechanical and thermal stability, and, most importantly, the ease of functionalization have made these materials an attractive candidate for drug delivery by encapsulating or attaching drugs to their exterior surfaces.[6,25–27] Furthermore, the small size of these systems allows them to move more easily throughout the human body than larger materials. Drug delivery using carbon nanostructures has been widely investigated as a possible strategy for reducing toxicity and side effects, as well as improving therapeutic efficacy in cancer treatment.[28–30] For example, extensive experimental[31–33] and theoretical studies[34–36] have revealed that different carbon nanostructures, such as carbon nanotubes, fullerenes, and graphene, have a considerable advantage in the treatment of various diseases due to their high drug loading capacity, long circulation time, and short desorption times. Moreover, density functional theory (DFT) studies showed that the addition of impurities by chemical doping may offer additional active sites to establish intermolecular interactions between the drug and the nanocarrier, and

[a]Department of Chemistry, Faculty of Basic Sciences, University of Maragheh, P. O. Box 55136-553, Maragheh, Iran. E-mail: esrafili@maragheh.ac.ir
[b]Centre for Computational Materials Science, University of Malakand, Chakdara, Pakistan
[c]Department of Chemistry, University of Malakand, Chakdara, Pakistan

† Electronic supplementary information (ESI) available. See DOI: 10.1039/d1ra09153k

noncovalent interactions were the primary drivers for drug loading and release.[37–39] The functionalization of carbon nanostructures with various metal atoms has been also utilized to trigger and regulate drug loading/releasing in order to adsorption properties of drugs. For example, a recent quantum mechanics investigation based on DFT calculations[40] have revealed that doping C_{60} fullerene with a B atom can transform this inert material into an active and promising material for delivering aspirin molecules in a water medium.

5-Fluorouracil (5FU) is an antimetabolite chemotherapeutic medication that is widely used to treat colorectal, breast, head and neck, pancreatic, and stomach cancers.[41–43] Because 5FU is a water-soluble medication, it is administrated intravenously. However, the emergence of drug resistance is a significant restriction in the therapeutic use of 5FU. For example, because of its poor bioavailability, 5FU cure rates for advanced colorectal cancer are fewer than 15%.[42] Furthermore, 5FU causes significant toxicological damage to the gastrointestinal system and blood factors, as well as neurological, dermatological, and cardiological responses.[41,44] Thus, potential DDSs for 5FU must be developed in order to provide a greater therapeutic impact with less adverse effects. For example, previous DFT studies investigated the feasibility of different nanostructures for 5FU adsorption and delivery, such as carbon fullerenes and nanotubes or their BN analogues.[45–47] However, one important weakness of these DFT works is that they only investigate the adsorption of a single 5FU molecule. Given the high surface-to-volume ratio of nanostructures, determining the maximum capacity of loading the 5FU over these systems would be very interesting.

The drug loading process is a very important component in DDSs that impacts therapeutic efficiency. It is commonly accepted that DDSs are based on reversible interactions between nanocarrier and drug, as such interactions facilitate drug release to the target cell.[48,49] Noncovalent interactions like as van der Waals contacts, electrostatic interactions, hydrogen bonding, and π–π staking interactions are considered to be driving forces in drug delivery *via* nanostructures.[50,51] Noncovalent interactions between drug and nanocarrier not only preserve the drug's purity but also improves therapeutic efficacy by boosting cellular uptake. As a result, investigating the nature of the drug–nanocarrier interaction and the mutual effect of the drug and nanocarrier is critical for the design and development of novel DDSs.

The main objective of this study is to investigate the potential of alkali metal decorated C_{60} fullerenes (AM/C_{60}; AM = Li, Na, K) as a viable drug delivery vehicle for the 5FU drug. Dispersion-corrected DFT calculations are conducted to investigate the adsorption energies, charge transfers, and electronic structure of 5FU molecules adsorbed onto AM/C_{60} systems. The solvation effects on the adsorption energies of 5FU molecules are thoroughly studied. The results show that a C_{60} fullerene may be stably decorated with 12 Li and 6 Na or K atoms, and that each of these AM atoms can carry a 5FU molecule. The short desorption times and modest adsorption energies obtained indicate that AM/C_{60} fullerenes are ideal systems for the delivery of 5FU molecules.

2. Computational aspects

AM/C_{60} fullerenes were prepared by depositing AM atoms on the outer surface of pristine C_{60}. The dispersion-corrected PBE-D2 (ref. 52 and 53) density functional was used in conjunction with a double numerical plus polarization function (DNP) basis set to minimize the structures. During the geometry optimizations, all atoms were free to move. A Fermi smearing of 0.005 Ha to the orbital occupancy was set to improve computational performance. All DFT calculations were performed within a cubic box with $a = b = c = 30$ Å. The solvent effects were included by the conductor-like screening model (COSMO)[54] method. All the DFT calculations were conducted by the DMol.[55,56]

To evaluate the stability of AM/C_{60} complexes, the adsorption energies of the AM atoms were calculated using the following equation:

$$E_{\text{ads}}\,(\text{AM}) = 1/n[E_{\text{decorated}} - E_{\text{C60}} - (n \times E_{\text{AM}})] \quad (1)$$

in which $E_{\text{decorated}}$, E_{C60} and E_{AM} are, respectively, the energies of AM/C_{60}, pristine C_{60} and a single AM atom. n is the number of the added AM atoms. Likewise, to examine the feasibility of AM/C_{60} fullerenes to adsorb 5FU molecules, the adsorption energy (E_{ads}) per 5FU was determined using the following equation:

$$E_{\text{ads}} = 1/m[E_{\text{complex}} - E_{\text{decorated}} - (m \times E_{\text{5FU}})] \quad (2)$$

where m is the number of adsorbed 5FU molecules; E_{complex} and $E_{\text{decorated}}$ are the total energies of the 5FU adsorbed and pristine AM/C_{60}, respectively, and E_{5FU} is the energy of a single 5FU.

To obtain the degree of electron density redistribution (EDR) caused by the formation of 5FU–fullerene complexes, the following equation was used:

$$\text{EDR} = \rho_{\text{complex}} - \sum_i \rho_i \quad (3)$$

in which the ρ_{complex} is the electron density of the complex, while ρ_i is the electron density of the subunits, all having the geometry as that in the complex.

3. Results and discussion

3.1. Pristine and AM decorated C_{60} fullerenes

Previous studies[21,57–61] have extensively investigated the geometry and electronic structure properties of pure C_{60}. It consists of twelve pentagons and twenty hexagons, with two types of C–C bonds: one shared by two neighboring hexagons (R_{66}) and the other by one pentagon and one hexagon (R_{65}). The optimized R_{66} and R_{65} bond distances in C_{60} are 1.40 and 1.45 Å, respectively, which differ from the C–C bond length in graphene (≈1.42 Å).[62] The charge density analysis reveals that the electronic charge is uniformly distributed throughout the C_{60}, and there is no dipole moment in this material due to its high symmetry. Though there are plentiful of sites for adsorption of AM atoms, our DFT calculations show that the above of the center of pentagon and hexagon rings are the most active adsorption sites for the AM atoms. As a result, we initially put

a single AM atom on the pentagon or hexagon rings of C_{60} to get the most stable geometry of AM/C_{60}. In the case of Li atom, it is revealed that the calculated adsorption energies on the center of a pentagon or a hexagon site differ by only 0.8 kcal mol^{-1}. In accordance with earlier studies,[63] the adsorption of the Li atom on the center of a hexagon is slightly more favorable. Likewise, the center of the hexagonal face is preferably the lowest energy binding site for the Na and K atoms (Fig. 1). From Table 1, one can see that the adsorption energies decrease as the size of the AM increases. The E_{ads} values of the Li, Na and K atom adsorbed on the C_{60} fullerene are calculated to be −43.58, −36.86 and −36.22 kcal mol^{-1}, respectively, which are in good agreement with those of other studies.[63–65] This also implies that the interaction between the C_{60} fullerene and the AM atoms is rather strong. As a result, the C–C bond distances of the interacting hexagon ring are slightly elongated after the adsorption of the AM atom. Taking the Li/C_{60} as an example, the R_{65} and R_{66} distances of the fullerene increase by 0.01 and 0.02 Å, respectively, upon the Li adsorption. According to the Hirshfeld analysis, the charge on the AM atoms increases as their size grows. Though this observation is compatible with the reactivity of these atoms, it is not entirely consistent with the order of their adsorption energies. A similar discrepancy in charge transfer and adsorption energies of the AM atoms has been reported in several related investigations,[64] as well as for AM/B_{80} complexes.[66] It is most likely due to a more appropriate back-bonding interaction between the empty 2p states of the Li and the filled 2p states of the surrounding C atoms, which strengthens the Li–C interaction at the price of a smaller positive charge induced on the Li atom. A similar, albeit weaker, mechanism is also predicted for the Na/C_{60}. Nonetheless, the presence of a significant positive charge on the AM atoms suggests a strong propensity for interaction with electron-rich species. The EDR analysis is used to gain a better understanding of the mutual polarization of the AM and C_{60} moieties during the formation of AM/C_{60} complexes. The approach of the

Table 1 Calculated adsorption energies per AM atom (E_{ads}, kcal mol^{-1}), average Hirshfeld charge on the AM atom (Q_{AM}, |e|) and HOMO(SOMO)–LUMO energy gap (eV) of the AM decorated C_{60} fullerenes

Species	E_{ads}	Q_{AM}	HOMO(SOMO)–LUMO gap
Li/C_{60}	−43.58	0.47	1.48
Na/C_{60}	−36.86	0.62	1.50
K/C_{60}	−36.22	0.70	1.51
Li_{12}/C_{60}	−41.05	0.33	1.05
Na_6/C_{60}	−31.27	0.51	0.91
K_6/C_{60}	−30.90	0.59	0.89

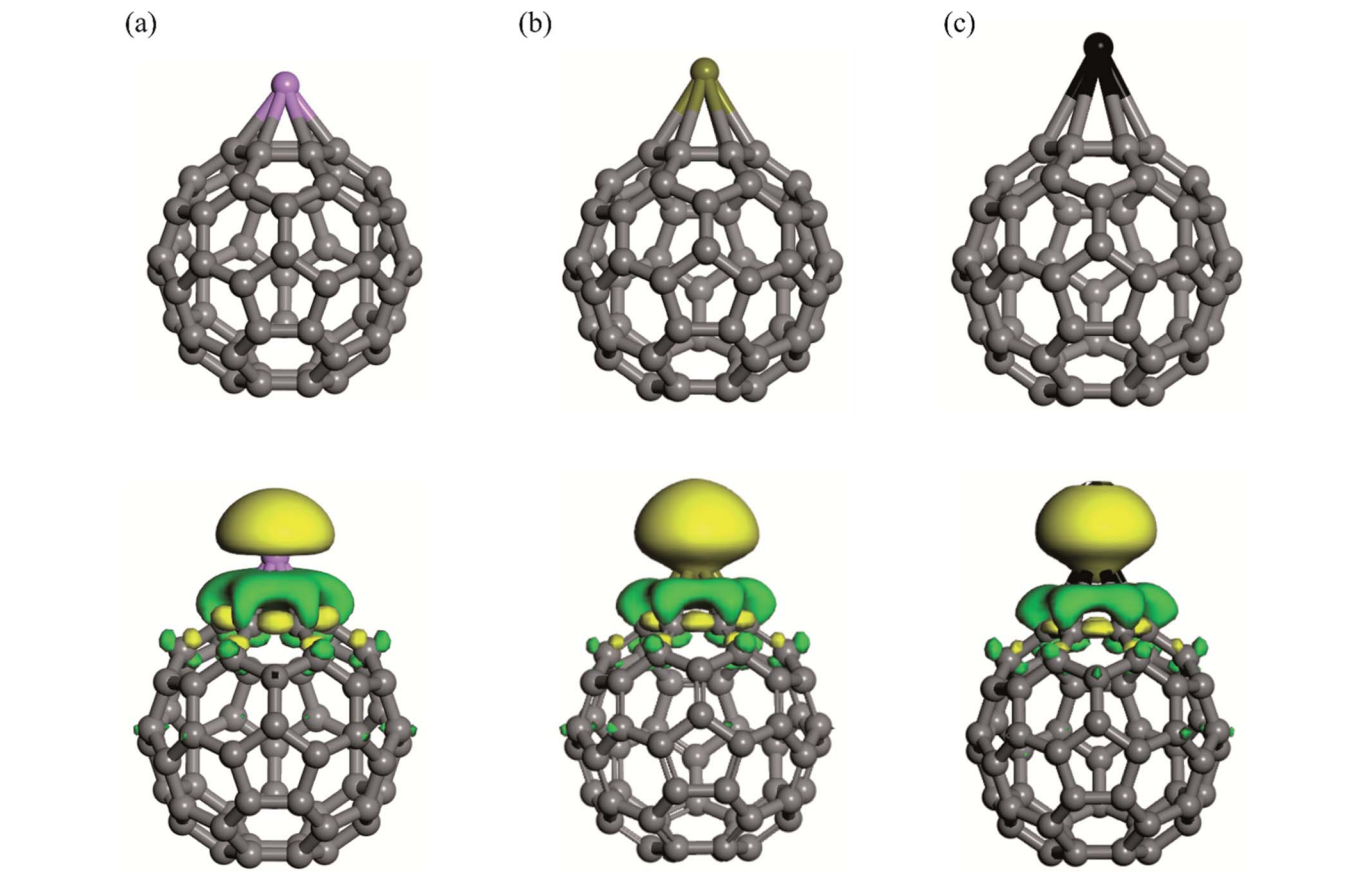

Fig. 1 The relaxed structure (above) and EDR isosurface (below, isovalue = 0.01 au) of (a) Li/C_{60}, (b) Na/C_{60} and (c) K/C_{60}. In the EDR isosurfaces, the gain and loss electron density areas are shown in green and yellow, respectively.

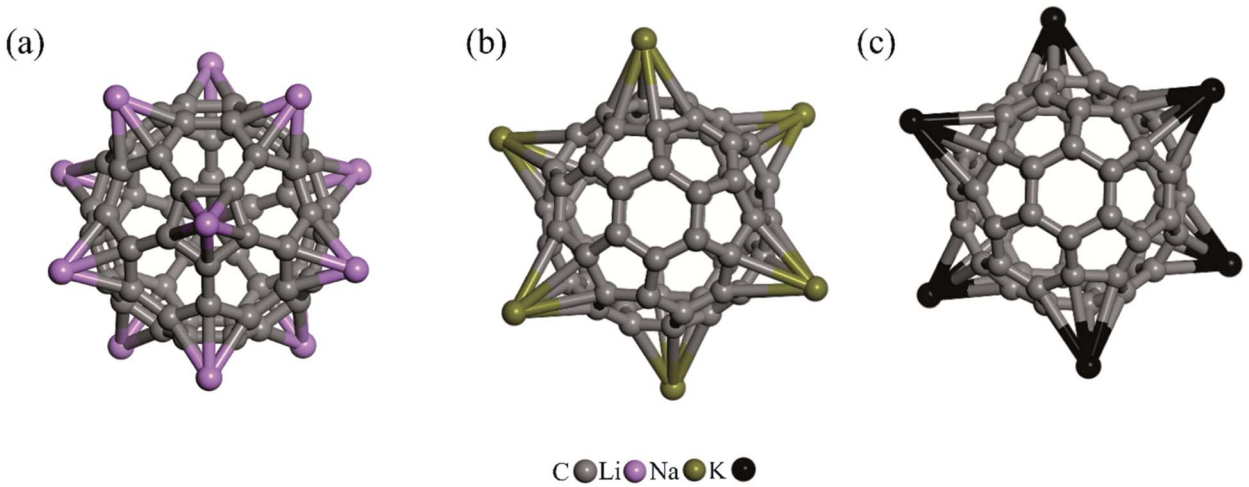

Fig. 2 The optimized structures of (a) Li_{12}/C_{60}, (b) Na_6/C_{60} and (c) K_6/C_{60} fullerenes.

AM atom to the C_{60} produces a significant electron density loss region on the AM atom, indicating its polarization in the presence of C_{60} (see Fig. 1). Likewise, the presence of the AM atom results in an area of increased electron density on the C_{60}. It is worth noting that the emergence of such electron gain/loss areas can contribute to increased electrostatic attraction between the AM atom and C_{60}, and hence the stability of the AM/C_{60} complex. Furthermore, the degree of the charge density difference in the AM/C_{60} systems is affected by the nature of the AM atom and becomes more significant as the size of the AM atom increases (Li < Na < K).

The number of AM atoms that a C_{60} molecule may adsorb is a crucial topic here. This is significant because it enables maximum capacity for delivering 5FU molecules using only one C_{60}. Therefore, additional AM atoms are added to the C_{60} in order to find the maximum coverage of these atoms. It should be noted that the cohesive energies of bulk Li, Na, and K are 37.8, 25.6, and 21.6 kcal mol^{-1},[67] respectively, and thus the absolute value of average adsorption energy should be greater than these cohesive energies to avoid the "clustering" of AM atoms. Fig. 2 depicts the maximum number of AM atoms that C_{60} fullerene can hold before clustering occurs. Consistent with previous DFT calculations,[68,69] it is found that when additional Li atoms are added to the fullerene, the pentagonal face definitely becomes the favored site. Indeed, as seen in Fig. S1 of the ESI,† the energy barrier for the migration of the Li atom from the hexagon ring into the neighboring pentagon is about 10 kcal mol^{-1}. As a result, a maximum of 12 Li atoms can be adsorbed on pure C_{60} with an adsorption energy of −41.05 eV per Li atom (Table 1). However, in the case of Na and K, a maximum of 6 atoms may be attached to the C_{60} simultaneously, with average E_{ads} values of −31.27 and −30.90 kcal mol^{-1}, respectively. It is worth noting that the average adsorption energies of the AM atoms in Li_{12}/C_{60}, Na_6/C_{60}, or K_6/C_{60} are less than those of a single AM atom adsorbed structures, which can be attributed to a decrease in the electron affinity of the C_{60} fullerene with stepwise addition of the AM atom. Meanwhile, the positive charge on the AM atoms decrease when more AM atoms are deposited over the C_{60} fullerene.

We also performed *ab initio* molecular dynamics (MD) simulations at $T = 300$ K for 5000 fs to assess the stability of the obtained Li_{12}/C_{60}, Na_6/C_{60}, and K_6/C_{60} systems. As seen in Fig. S2 of the ESI,† the AM decorated fullerenes remain stable following the MD simulations. The AM atoms, in particular, stay on the C_{60} and no clustering occurs, indicating that these structures are stable at ambient temperatures. It is worth mentioning that the calculated energy gap between the highest occupied molecular orbital and the lowest unoccupied molecular orbital (HOMO–LUMO gap) of pure C_{60} is 1.64 eV. The addition of AM atoms changes the electronic structure of the C_{60} and reduces its HOMO–LUMO gap. Because AM atoms have an unpaired electron, the formation of AM/C_{60} complexes results in the development of a singly occupied molecular orbital (SOMO) around the Fermi level. As shown in Table 1, the energy gap between the SOMO and LUMO of Li/C_{60}, Na/C_{60} and K/C_{60} is 1.48, 1.50, and 1.51 eV, which is 0.16, 0.14, and 0.13 eV less than the HOMO–LUMO gap of C_{60}. Given that a narrow HOMO(SOMO)–LUMO gap indicates low kinetic stability,[70] this finding implies that AM/C_{60} complexes are more chemically reactive than pure C_{60}.

3.2. Adsorption of 5FU on pristine and AM decorated C_{60}

To evaluate the adsorption behavior of AM-decorated C_{60} fullerenes, a 5FU molecule is allowed to approach the exterior surfaces of these complexes. Consider the singly adsorbed AM complexes first. The optimized most stable structures of 5FU molecule absorbed on Li/C_{60}, Na/C_{60}, and K/C_{60} are shown in Fig. 3. Table 2 displays the adsorption energies and charge-transfer values of the 5FU molecule. According to our DFT calculations, the 5FU prefers to attach to the decorated AM atom from its O site. The binding distance between the drug molecule and AM/C_{60} is determined to be 1.82, 2.19, and 2.60 Å for AM = Li, Na, and K, respectively. The adsorption energy of the 5FU is −19.33, −16.58 and −14.07 kcal mol^{-1} on Li/C_{60}, Na/

C_{60} and K/C_{60}, respectively, which falls within the range of chemisorption. The E_{ads} values of the 5FU molecule decrease as the size of the AM atom increases, which is inconsistent with the degree of polarization and the Hirshfeld charge on these atoms. It should be noticed that the calculated E_{ads} values of the 5FU are more negative than those calculated on other surfaces such as $B_{24}N_{24}$ (−11.90 kcal mol^{-1})[45] and Ge-doped BN nanotubes (−12.20 kcal mol^{-1}).[47] The 5FU molecule serves as the electron donor in all optimized complexes, with a charge-transfer value of 0.20, 0.13, and 0.08 electrons for AM = Li, Na, and K, respectively. These findings clearly show that, in addition to electrostatic attraction between positively charged AM atom and negatively charged O atoms of 5FU, orbital interactions also play an essential role in the formation of these

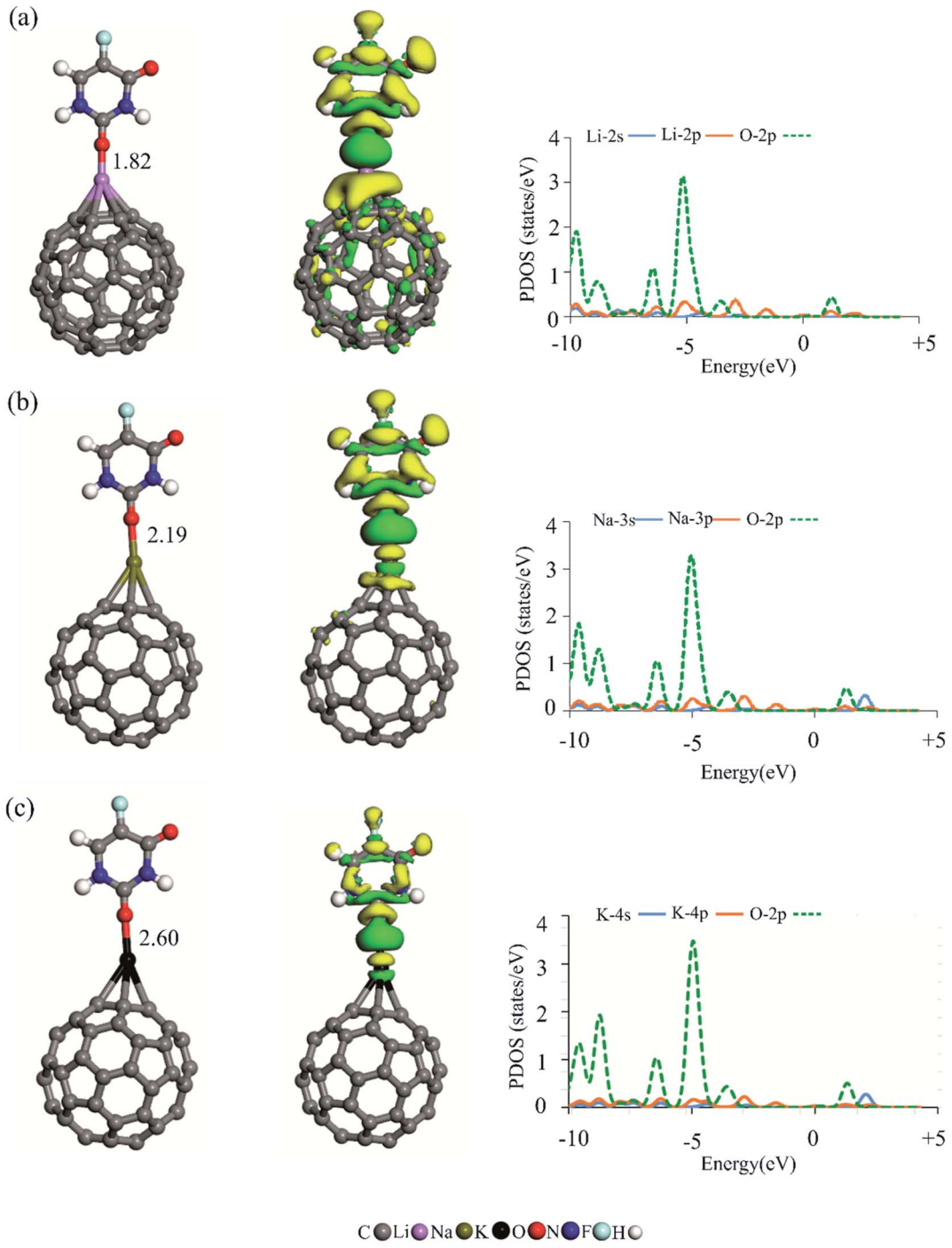

Fig. 3 The relaxed structure (left), corresponding EDR isosurface (middle, isovalue = 0.01 au) and PDOS plots (right) of the 5FU molecule adsorbed on (a) Li/C_{60}, (b) Na/C_{60} and (c) K/C_{60}. All bond distances are in Å. In the EDR isosurfaces, the gain and loss electron density areas are shown in green and yellow, respectively. The Fermi energy is set to zero in the PDOS plots.

Table 2 Calculated adsorption energies (E_{ads}, kcal mol^{-1}), charge-transfer (Q_{CT}, |e|) and desorption times (τ, s) per adsorbed 5FU molecule on AM/C_{60} fullerenes in the gas phase

Species	E_{ads}	Q_{CT}	τ
Li/C_{60}	−19.33	0.20	147.50
Na/C_{60}	−16.58	0.13	1.42
K/C_{60}	−14.07	0.08	0.02
Li_{12}/C_{60}	−16.06	0.16	0.59
Na_6/C_{60}	−14.69	0.09	0.06
K_6/C_{60}	−12.34	0.06	<0.01

complexes. In fact, the adsorption energies are well correlated with the amount of the charge-transfer values between the 5FU and the AM/C_{60} fullerenes, suggesting that the charge-transfer is more essential for the stability of these complexes than the electrostatic interactions. This is confirmed further by the PDOS analysis, which shows that there is substantial overlap between the empty p orbital of the AM atom and the O-2p orbitals of the drug molecule around the Fermi level. Note that compared to Na/C_{60} and K/C_{60}, the degree of such orbital overlap is more important in Li/C_{60}.

To get additional information about the charge density rearrangement upon the adsorption of 5FU on AM/C_{60} systems, the EDR analysis is performed. Fig. 3 shows the obtained iso-surfaces, with the gain and loss electron density areas shown in green and yellow, respectively. As seen, the adsorption of 5FU is associated with a considerable charge density rearrangement around the interacting atoms, suggesting that the mutual polarization of 5FU and AM/C_{60} subunits upon the complex formation. In particular, the appearance of a large electron density loss region on the 5FU confirms that this molecule serves as the electron donor. Note also that the amount of the charge density rearrangement is not same for these complexes; the stronger interaction between the 5FU and Li/C_{60} induces a more substantial rearrangement of the electron density. That is to say, the EDR analysis can be used as a suitable tool for assessing the adsorption strength between the 5FU molecule and AM/C_{60} fullerenes.

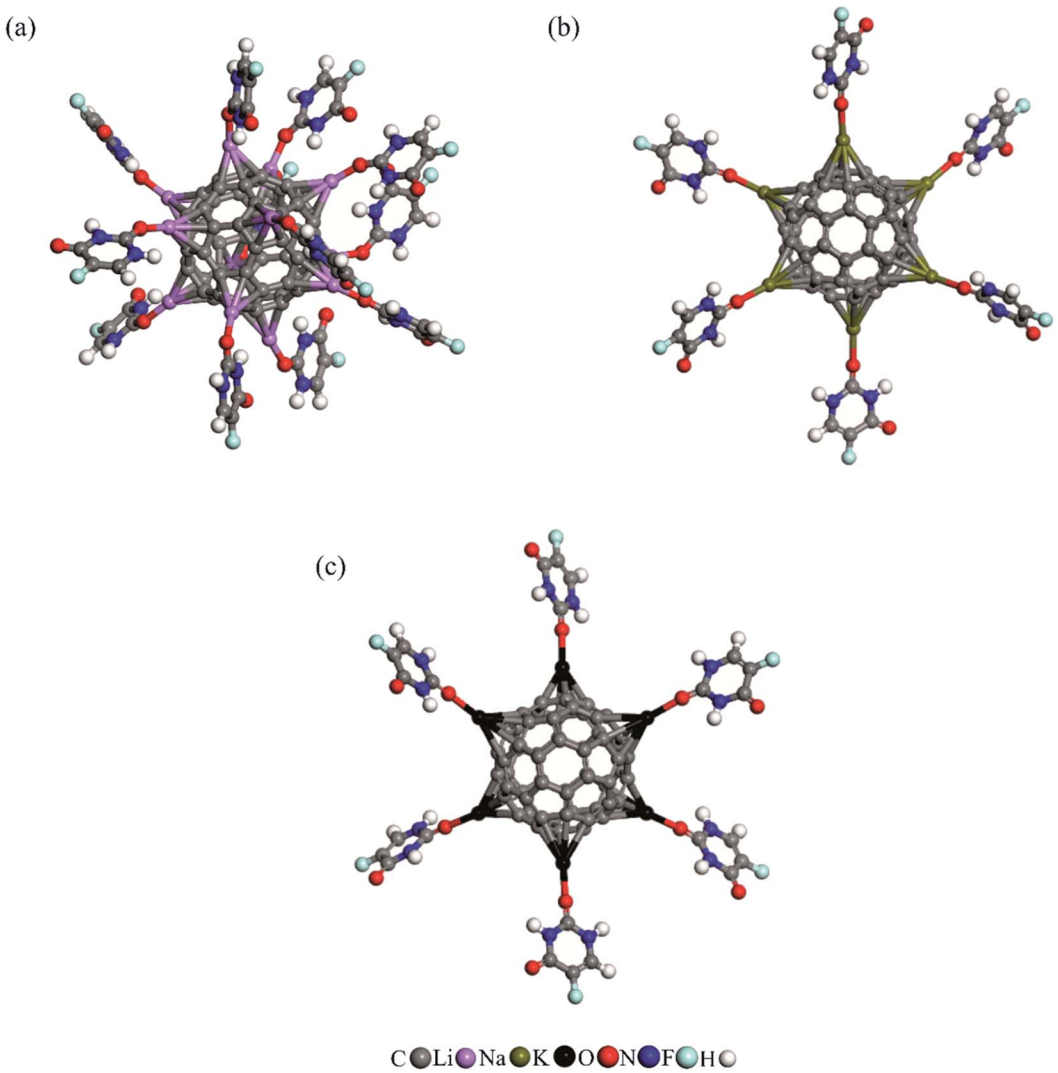

Fig. 4 (a) The optimized geometries of 5FU molecules adsorbed on (a) Li_{12}/C_{60}, (b) Na_6/C_{60} and K_6/C_{60} fullerenes.

Using the above information, we placed a 5FU molecule on each AM atom of Li_{12}/C_{60}, Na_6/C_{60}, and K_6/C_{60} and relaxed the resulting complexes. Fig. 4 illustrates the optimized structures of the derived complexes, and Table 2 lists the adsorption energies and charge-transfer values. The calculated adsorption energies per 5FU are −16.06, −14.69, and −12.34 kcal mol^{-1}, indicating that the AM atoms in these systems can efficiently adsorb 5FU molecules. Due to repulsion effects between the adsorbed 5FU molecules, these average E_{ads} values are slightly lower than the E_{ads} value on the single AM decorated C_{60}.

3.3. Drug release

Although the drug molecule must be stably adsorbed on the host material for effective drug delivery, this adsorption must not be so strong that it makes drug desorption difficult. As previously mentioned, the calculated adsorption energies of 5FU on the AM decorated C_{60} fullerenes range between −12.34 and −19.33 kcal mol^{-1}, which is neither too strong nor too weak. That is, the decorated systems may be able to desorb the 5FU molecule due to the modest adsorption energies. However, as the ambient temperature rises, the 5FU bonding with the decorated AM atoms is expected to weaken owing to entropic effects. Hence, to more accurately assess this, the desorption time (τ) for the 5FU molecule is calculated using the following equation:[72]

$$\tau = \nu^{-1} \exp\left(\frac{E_{ads}}{k_B T}\right) \quad (4)$$

where k_B is the Boltzmann constant, T is the ambient temperature (298.15 K), ν is a factor of 10^{12} Hz, and E_{ads} is the adsorption energy. According to the above equation, the drug's adsorption energy has an exponential relationship with its desorption time. From Table 2, the estimated τ values for 5FU desorption from Li/C_{60}, Na/C_{60}, and K/C_{60} fullerenes are 147.50, 1.42, and 0.02 seconds, respectively, which is short enough to release the drug from the fullerene surface. The average desorption time for the Li_{12}/C_{60}, Na_6/C_{60}, and K_6/C_{60} systems have even shorter desorption times. As a consequence, the reversible adsorption of 5FU on AM decorated fullerenes may be deduced.

The 5FU, on the other hand, is intended to be delivered into cancerous cells. However, it is generally known that cancerous cells have a pH value less than that of normal cells (pH < 7).[71] As a result, it is reasonable to anticipate that when the 5FU reaches the target cancer cell, it will react with the proton ion. To demonstrate this, we added a proton to different regions of the adsorbed 5FU molecule. Following careful geometry optimization, it is found that the proton is attached to the bridge O atom as a result of the larger negative charge concentrated on this atom (Fig. 5). As can be seen, the addition of the proton increases the binding distance of the 5FU relative to its neutral form. The calculated adsorption energies of protonated 5FU on Li/C_{60}, Na/C_{60}, and K/C_{60} fullerenes are −7.75, −5.64, and −3.90 kcal mol^{-1}, respectively. Clearly, these E_{ads} values are much smaller than those of neutral 5FU, indicating that the drug molecule can be readily separated from the fullerene when it reaches the targeted cancerous cell.

3.4. Solvent effects

The solvation energies (E_{solv}) of the 5FU complexes with the AM anchored C_{60} fullerenes are calculated to determine drug solubility in the aqueous environment. The solvation energy is

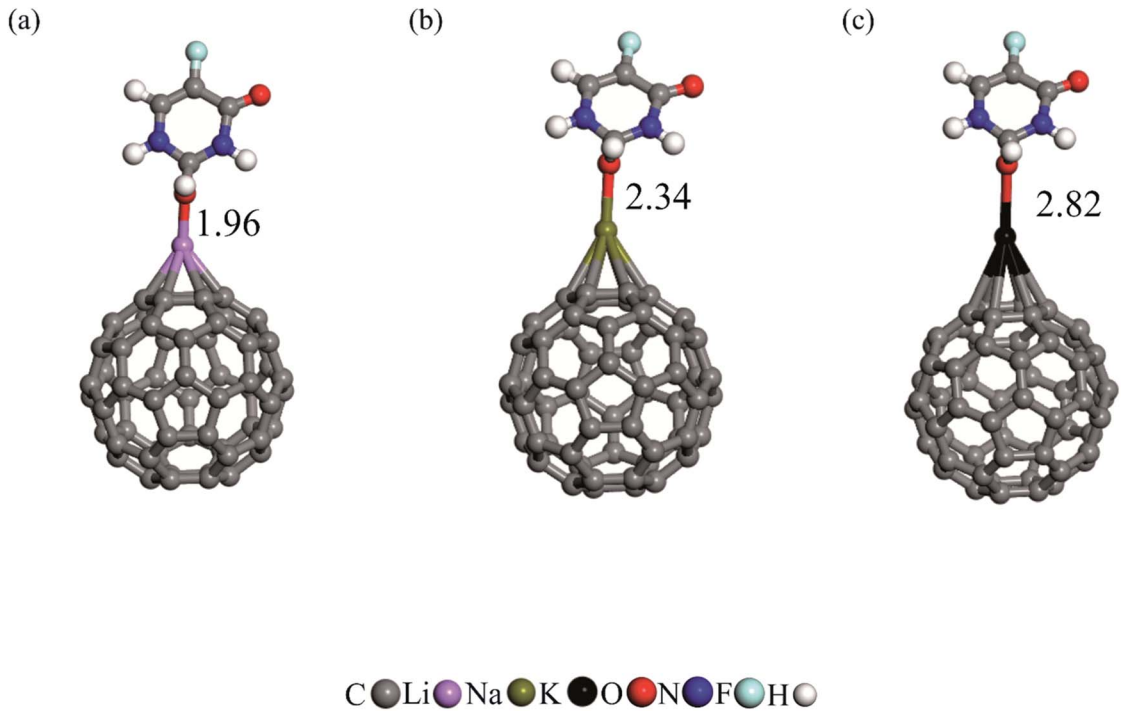

Fig. 5 The adsorption of protonated 5FU on (a) Li/C_{60}, (b) Na/C_{60} and (c) K/C_{60}. All bond distances are in Å.

Table 3 Calculated adsorption energies (E_{ads}, kcal mol^{-1}), charge-transfer (Q_{CT}, |e|) and desorption times (τ, s) per adsorbed 5FU molecule on AM/C_{60} fullerenes in the aqueous phase

Species	E_{solv}	E_{ads}	Q_{CT}	τ
Li/C_{60}	−30.70	−13.73	0.14	1.17×10^{-2}
Na/C_{60}	−35.20	−9.24	0.11	5.97×10^{-6}
K/C_{60}	−35.90	−8.50	0.05	1.71×10^{-6}
Li_{12}/C_{60}	−11.74	−10.85	0.11	9.06×10^{-5}
Na_6/C_{60}	−23.87	−8.10	0.05	8.71×10^{-7}
K_6/C_{60}	−24.58	−6.88	0.03	1.11×10^{-7}

defined here as the difference between the total energy of the complexes in the gas and aqueous phases. Moreover, the adsorption energies and related charge-transfer values owing to the adsorption of 5FU on the decorated fullerenes are obtained in order to further analyze the solvation effects. Table 3 summarizes the obtained solvation energies, adsorption energies, charge-transfer and desorption time values per 5FU molecule. It is seen that the E_{solv} values are all negative, implying that the solvation of the derived complexes tends to stabilize these systems. As the size of the AM atom gets bigger, the solvation effects become more significant. When the adsorption energy values are considered, it is evident that the presence of water molecules tends to decrease the adsorption strength of the 5FU. This is because the solvation energies of bare AM/C_{60} fullerenes are larger than those of 5FU-AM/C_{60} adsorbed complexes due to the more polar AM-C bonds. The Hirshfeld study supports this conclusion, with calculated charge-transfer values in the aqueous medium are smaller than those in the gas phase. According to eqn (4), the incorporation of solvation effects can reduce the desorption time of 5FU molecules from AM decorated fullerenes. Hence, it may be inferred that the release of 5FU can be promoted inside the aqueous solution.

4. Conclusions

In summary, a dispersion-corrected DFT investigation of the capability of AM decorated C_{60} fullerenes (AM/C_{60}; AM = Li, Na, and K) was conducted. It was found that the AM atom may be decorated stably on the hexagon rings of C_{60} fullerene. The MD simulations revealed that the AM-decorated fullerenes are thermally stable. The decorated AM atoms in AM/C_{60} can serve as active sites for the adsorption of 5FU molecules. Our findings indicated that Li decorated C_{60} fullerene can adsorb up to 12 5FU molecules with an average adsorption energy of −16.06 kcal mol^{-1}. In the case of the Na and K decorated systems, the results showed that a maximum of 6 Na or K may bind to the C_{60}, each of which can adsorb one 5FU molecule. The E_{ads} values for the adsorption of a protonated 5FU molecule are significantly smaller than those for a neutral one, suggesting that the drug molecule can be easily detached from the fullerene when it reaches the cancerous cell. The addition of solvent effects reduces the strength of 5FU-fullerene complexes, suggesting that the drug release process might be assisted by solvent molecules. This work demonstrated for the first time how the decorating of C_{60} fullerene with AM atoms may significantly improve the capability of this system for delivering multiple 5FU molecules.

Conflicts of interest

There are no conflicts to declare.

References

1 V. V. Ranade and J. B. Cannon, *Drug delivery systems*, CRC Press, 2011.
2 C. Li, J. Wang, Y. Wang, H. Gao, G. Wei, Y. Huang, H. Yu, Y. Gan, Y. Wang and L. Mei, *Acta Pharm. Sin. B*, 2019, **9**, 1145–1162.
3 M. Naeem, U. A. Awan, F. Subhan, J. Cao, S. P. Hlaing, J. Lee, E. Im, Y. Jung and J.-W. Yoo, *Arch. Pharmacal Res.*, 2020, **43**, 153–169.
4 Y. K. Sung and S. W. Kim, *Biomater. Res.*, 2020, **24**, 1–12.
5 S. Senapati, A. K. Mahanta, S. Kumar and P. Maiti, *Signal Transduction Targeted Ther.*, 2018, **3**, 1–19.
6 Q. Guo, X.-t. Shen, Y.-y. Li and S.-q. Xu, *Curr. Med. Sci.*, 2017, **37**, 635–641.
7 Z. Li, A. L. B. de Barros, D. C. F. Soares, S. N. Moss and L. Alisaraie, *Int. J. Pharm.*, 2017, **524**, 41–54.
8 G. Karthivashan, P. Ganesan, S.-Y. Park, J.-S. Kim and D.-K. Choi, *Drug Delivery*, 2018, **25**, 307–320.
9 J. Kaur, G. S. Gill and K. Jeet, *Characterization and Biology of Nanomaterials for Drug Delivery*, Elsevier, 2019, pp. 113–135.
10 N. Zahin, R. Anwar, D. Tewari, M. Kabir, A. Sajid, B. Mathew, M. Uddin, L. Aleya and M. M. Abdel-Daim, *Environ. Sci. Pollut. Res.*, 2020, **27**, 19151–19168.
11 X. Chen, R. Tong, Z. Shi, B. Yang, H. Liu, S. Ding, X. Wang, Q. Lei, J. Wu and W. Fang, *ACS Appl. Mater. Interfaces*, 2018, **10**, 2328–2337.
12 C. J. M. Rivas, M. Tarhini, W. Badri, K. Miladi, H. Greige-Gerges, Q. A. Nazari, S. A. G. Rodríguez, R. Á. Román, H. Fessi and A. Elaissari, *Int. J. Pharm.*, 2017, **532**, 66–81.
13 R. Kanwar, J. Rathee, D. B. Salunke and S. K. Mehta, *ACS Omega*, 2019, **4**, 8804–8815.
14 M. Saeedi, M. Eslamifar, K. Khezri and S. M. Dizaj, *Biomed. Pharmacother.*, 2019, **111**, 666–675.
15 M. Mir, S. Ishtiaq, S. Rabia, M. Khatoon, A. Zeb, G. M. Khan, A. ur Rehman and F. ud Din, *Nanoscale Res. Lett.*, 2017, **12**, 1–16.
16 J.-F. Hsu, S.-M. Chu, C.-C. Liao, C.-J. Wang, Y.-S. Wang, M.-Y. Lai, H.-C. Wang, H.-R. Huang and M.-H. Tsai, *Cancers*, 2021, **13**, 195.
17 N. Martín, T. Da Ros and J.-F. Nierengarten, *J. Mater. Chem. B*, 2017, **5**, 6425–6427.
18 H. G. Shiraz and M. G. Shiraz, *Int. J. Hydrogen Energy*, 2017, **42**, 11528–11533.
19 Y. Tang, J. Zhou, Z. Shen, W. Chen, C. Li and X. Dai, *RSC Adv.*, 2016, **6**, 93985–93996.
20 E. Ashori, F. Nazari and F. Illas, *Phys. Chem. Chem. Phys.*, 2017, **19**, 3201–3213.

21 M. D. Esrafili and H. Janebi, *Mol. Phys.*, 2020, **118**, e1631495.
22 W. Huang, M. Shi, H. Song, Q. Wu, X. Huang, L. Bi, Z. Yang and Y. Wang, *Chem. Phys. Lett.*, 2020, **758**, 137940.
23 M. D. Esrafili, A. A. Khan and P. Mousavian, *RSC Adv.*, 2021, **11**, 22598–22610.
24 E. Shakerzadeh and L. Azizinia, *Chem. Phys. Lett.*, 2021, **764**, 138241.
25 S. Kraszewski, E. Duverger, C. Ramseyer and F. Picaud, *J. Chem. Phys.*, 2013, **139**, 174704.
26 E. Alipour, F. Alimohammady, A. Yumashev and A. Maseleno, *J. Mol. Model.*, 2020, **26**, 1–8.
27 M. Kumar and K. Raza, *Pharm. Nanotechnol.*, 2017, **5**, 169–179.
28 R. Maleki, A. Khoshoei, E. Ghasemy and A. Rashidi, *J. Mol. Graphics Modell.*, 2020, **100**, 107660.
29 J. Saleem, L. Wang and C. Chen, *Adv. Healthcare Mater.*, 2018, **7**, 1800525.
30 F. Niazvand, P. R. Wagh, E. Khazraei, M. B. Dastjerdi, C. Patil and I. A. Najar, *J. Compos. Compd.*, 2021, **3**, 140–151.
31 S. Augustine, J. Singh, M. Srivastava, M. Sharma, A. Das and B. D. Malhotra, *Biomater. Sci.*, 2017, **5**, 901–952.
32 B. Hosnedlova, M. Kepinska, C. Fernandez, Q. Peng, B. Ruttkay-Nedecky, H. Milnerowicz and R. Kizek, *Chem. Rec.*, 2019, **19**, 502–522.
33 M. Serda, G. Szewczyk, O. Krzysztyńska-Kuleta, J. Korzuch, M. Dulski, R. Musioł and T. Sarna, *ACS Biomater. Sci. Eng.*, 2020, **6**, 5930–5940.
34 A. Hosseinian, E. Vessally, S. Yahyaei, L. Edjlali and A. Bekhradnia, *J. Cluster Sci.*, 2017, **28**, 2681–2692.
35 C. Parlak and Ö. Alver, *J. Mol. Struct.*, 2019, **1184**, 110–113.
36 H. Xu, X. Tu, G. Fan, Q. Wang, X. Wang and X. Chu, *J. Mol. Liq.*, 2020, **318**, 114315.
37 D. Shahabi and H. Tavakol, *Appl. Surf. Sci.*, 2017, **420**, 267–275.
38 R. Bagheri, M. Babazadeh, E. Vessally, M. Es' haghi and A. Bekhradnia, *Inorg. Chem. Commun.*, 2018, **90**, 8–14.
39 I. Ravaei, M. Haghighat and S. Azami, *Appl. Surf. Sci.*, 2019, **469**, 103–112.
40 F. Nattagh, S. Hosseini and M. D. Esrafili, *J. Mol. Liq.*, 2021, 117459.
41 J. D. Sara, J. Kaur, R. Khodadadi, M. Rehman, R. Lobo, S. Chakrabarti, J. Herrmann, A. Lerman and A. Grothey, *Ther. Adv. Med. Oncol.*, 2018, **10**, 1758835918780140.
42 K. R. Stefaniak, C. C. Epley, J. J. Novak, M. L. McAndrew, H. D. Cornell, J. Zhu, D. K. McDaniel, J. L. Davis, I. C. Allen and A. J. Morris, *Chem. Commun.*, 2018, **54**, 7617–7620.
43 P. Alvarez, J. A. Marchal, H. Boulaiz, E. Carrillo, C. Vélez, F. Rodriguez-Serrano, C. Melguizo, J. Prados, R. Madeddu and A. Aranega, *Expert Opin. Ther. Pat.*, 2012, **22**, 107–123.
44 E. Carrillo, S. A. Navarro, A. Ramírez, M. Á. García, C. Griñán-Lisón, M. Perán and J. A. Marchal, *Expert Opin. Ther. Pat.*, 2015, **25**, 1131–1144.
45 M. K. Hazrati, Z. Javanshir and Z. Bagheri, *J. Mol. Graphics Modell.*, 2017, **77**, 17–24.
46 M. Vatanparast and Z. Shariatinia, *J. Fluorine Chem.*, 2018, **211**, 81–93.
47 A. Soltani, M. T. Baei, E. T. Lemeski, S. Kaveh and H. Balakheyli, *J. Phys. Chem. Solids*, 2015, **86**, 57–64.
48 M. K. Hazrati, Z. Bagheri and A. Bodaghi, *Phys. E*, 2017, **89**, 72–76.
49 U. Srimathi, V. Nagarajan and R. Chandiramouli, *J. Mol. Liq.*, 2018, **265**, 199–207.
50 J. Ding, L. Chen, C. Xiao, L. Chen, X. Zhuang and X. Chen, *Chem. Commun.*, 2014, **50**, 11274–11290.
51 T. Doane and C. Burda, *Adv. Drug Delivery Rev.*, 2013, **65**, 607–621.
52 J. P. Perdew, K. Burke and M. Ernzerhof, *Phys. Rev. Lett.*, 1996, **77**, 3865–3868.
53 S. Grimme, *J. Comput. Chem.*, 2004, **25**, 1463–1473.
54 A. Klamt and G. Schüürmann, *J. Chem. Soc., Perkin Trans. 2*, 1993, 799–805.
55 B. Delley, *J. Chem. Phys.*, 1990, **92**, 508–517.
56 B. Delley, *J. Chem. Phys.*, 2000, **113**, 7756–7764.
57 A. E. Mahdy, *Mol. Phys.*, 2015, **113**, 3531–3544.
58 M. K. Hazrati and N. L. Hadipour, *Phys. Lett. A*, 2016, **380**, 937–941.
59 A. A. Khan, I. Ahmad and R. Ahmad, *Chem. Phys. Lett.*, 2020, **742**, 137155.
60 M. D. Esrafili and S. Heidari, *ChemistrySelect*, 2019, **4**, 4308–4315.
61 M. D. Esrafili and S. Heydari, *ChemistrySelect*, 2019, **4**, 2267–2274.
62 M. D. Esrafili and P. Mousavian, *Appl. Surf. Sci.*, 2018, **455**, 808–814.
63 A. Omidvar and A. Mohajeri, *Int. J. Hydrogen Energy*, 2017, **42**, 12327–12338.
64 K. Chandrakumar and S. K. Ghosh, *Nano Lett.*, 2008, **8**, 13–19.
65 D. S. De, J. A. Flores-Livas, S. Saha, L. Genovese and S. Goedecker, *Carbon*, 2018, **129**, 847–853.
66 Y. Li, G. Zhou, J. Li, B.-L. Gu and W. Duan, *J. Phys. Chem. C*, 2008, **112**, 19268–19271.
67 A. M. Halpern, *J. Chem. Educ.*, 2012, **89**, 592–597.
68 Q. Wang and P. Jena, *J. Phys. Chem. Lett.*, 2012, **3**, 1084–1088.
69 Q. Sun, P. Jena, Q. Wang and M. Marquez, *J. Am. Chem. Soc.*, 2006, **128**, 9741–9745.
70 J.-i. Aihara, *J. Phys. Chem. A*, 1999, **103**, 7487–7495.
71 G. Hao, Z. P. Xu and L. Li, *RSC Adv.*, 2018, **8**, 22182–22192.
72 J. Beheshtian, A. Ahmadi and Z. Bagheri, *Sens. Actuators, B*, 2012, **171**, 846–852.